Journal of Materials Chemistry C

PAPER

View Article Online
View Journal | View Issue

Cite this: J. Mater. Chem. C, 2018, 6, 4250

Non-doped white organic light-emitting diodes with superior efficiency/color stability by employing ultra-thin phosphorescent emitters†

Bo Zhao, *[a] Heng Zhang,[a] Ziqi Wang,[a] Yanqin Miao, [a] Zhongqiang Wang, [a] Jie Li, *[a] Hua Wang, [a] Yuying Hao [b] and Wenlian Li[c]

Received 9th January 2018,
Accepted 12th March 2018

DOI: 10.1039/c8tc00132d

rsc.li/materials-c

Using a simple method employing ultra-thin phosphorescent emitters into bis(3-(9,9-dimethyl-9,10-dihydroacridine)phenyl)sulfone (mSOAD) based on zig-zag acridine/sulfone derivative, high efficiency and high color stability of non-doped white organic light-emitting diodes (WOLEDs) are realized. After optimization of the location and quantity of the ultra-thin emitters, maximum current efficiency, power efficiency and external quantum efficiency (EQE) of the WOLEDs of 31.9 cd A^{-1}, 30.4 lm W^{-1} and 17.3%, respectively, are achieved. The stable white spectra are also obtained with the Commission Internationale de l'Eclairage (CIE) coordinates of (0.469 ± 0.008, 0.382 ± 0.004) from 4 V to 8 V. We find that efficient confinement to carriers and excitons has a key role; the location and quantity of ultra-thin emitters also have a large effect on device performance.

1. Introduction

White organic light-emitting diodes (WOLEDs) have received more and more attention due to their suitability for application in natural flat-panel light sources and flexible displays in solid state lighting. In general, WOLEDs are constructed by a multi-layer structure of blue/green/red or blue/orange emitting layers and high efficiency WOLEDs with ~20% external quantum efficiency (EQE) are usually obtained using fluorescent/phosphorescent hybrid or full phosphorescent materials. But it is undeniable that most of the WOLEDs are obtained using a host–guest doped system.

The host–guest doped system has to be applied in the emitting layer (EML) due to the high concentration quenching of the emitter, including the traditional fluorescent, phosphorescent and thermally activated delayed fluorescent (TADF) emitting materials.[1–4] Moreover, the host–guest doped system requires a multi-source heat deposition method, which also has some problems. For example, the concentration of the dopant is hard to control accurately and cross contamination would occur inevitably between different evaporator sources during the co-deposition process. Therefore, many research groups tried to develop highly efficient non-doped small molecular emitters.[5–11] Adachi's group exploited two non-doped pure organic emitters of blue (bis[4-(9,9-dimethyl-9,10-dihydroacridine)phenyl]sulfone, DMAC-DPS) and green (bis[4-(9,9-dimethyl-9,10-dihydroacridine)phenyl]methanone, DMAC-BP), which almost achieved an internal quantum efficiency (IQE) of 100%.[7] Tang's group also developed high-performance green non-doped OLEDs based on dibenzothiophene-benzoyl-9,9-dimethyl-9,10-dihydroacridine (DBT-BZ-DMAC) by combining aggregation-induced emission (AIE) and TADF.[8] The development of these non-doped small molecular fluorescent emitters provides a much larger platform to design high efficiency non-doped WOLEDs. Although there were some previous reports on the non-doped WOLEDs, they were focused on the application of ultra-thin red/green/blue emitters in the common hosts (TCTA, TPBi, Bepp2) or at the interface to form white light-emitting diodes.[12–20] Furthermore, the color stability based the non-doped WOLEDs need to be improved and the influence of the location and quantity of ultra-thin emitters on the device efficiency and spectra is rarely researched and also needs to be studied more.

In this work, we utilize a simple method instead of a host–guest doped system by employing an ultra-thin red phosphorescent emitter of iridium(III) bis(2-phenylquinoline) acetylacetonate

[a] Key Laboratory of Interface Science and Engineering in Advanced Materials of Ministry of Education, and Research Center of Advanced Materials Science and Technology, Taiyuan University of Technology, Taiyuan 030024, China. E-mail: zhaobo01@tyut.edu.cn, lijie01@tyut.edu.cn
[b] Key Laboratory of Advanced Transducers and Intelligent Control System of Ministry of Education, and College of Physics and Optoelectronics, Taiyuan University of Technology, Taiyuan 030024, China
[c] State Key Laboratory of Luminescence and Applications, Changchun Institute of Optics, Fine Mechanics and Physics, Chinese Academy of Sciences, Changchun 130033, China

† Electronic supplementary information (ESI) available. See DOI: 10.1039/c8tc00132d

($Ir(pq)_2acac$) and a blue fluorescent emitter of bis(3-(9,9-dimethyl-9,10-dihydroacridine)phenyl)sulfone (mSOAD) based on a zig-zag acridine/sulfone derivative to construct non-doped WOLEDs. By the optimization of different locations and quantities of an ultra-thin $Ir(pq)_2acac$ emitter, the non-doped WOLEDs with superior efficiency and color stability are finally obtained. The maximum current efficiency, power efficiency and EQE of 31.9 cd A^{-1}, 30.4 lm W^{-1} and 17.3%, respectively, are achieved. Meantime, the Commission Internationale de l'Eclairage (CIE) coordinates with a high color stability of (0.469 ± 0.008, 0.382 ± 0.004) from 4 V to 8 V are realized simultaneously. The location and quantity of ultra-thin emitters are also analyzed and we find they have a large effect on device performance.

2. Experimental section

2.1 Device fabrication

Device fabrication and performance characterization were performed following our previous reports.[21] All the WOLEDs were fabricated on glass substrates coated with indium tin oxide (ITO) and the sheet resistance was 10 Ω sq^{-1}. Before the ITO substrates were loaded into a high vacuum chamber (approximately 3×10^{-4} Pa) for subsequent deposition, the ITO substrates were cleaned with acetone, deionized water, acetone in sequence and then treated with ultraviolet-ozone for 15 min. After completion of the deposition of organic layers, the Al cathode with a shadow mask defining a device area of 3×3 mm^2 was deposited in the end.

2.2 Characterization

The photoluminescence (PL) and UV-Vis absorption spectra were measured using a FluoroMax-4 fluorescence spectrometer (HORIBA Jobin Yvon) and a Hitachi U-3900 scanning spectrophotometer, respectively. The electroluminescence (EL) spectra were measured using a PR-655 spectra scan spectrometer. The current–voltage–luminance curves were measured using a measuring system of a Keithley 2400 power supply combined with a BM-7A luminance colorimeter. EQE was calculated from the current density–voltage–luminance curve and EL spectra data. All the organic materials except for mSOAD were procured commercially without further purification. All the measurements

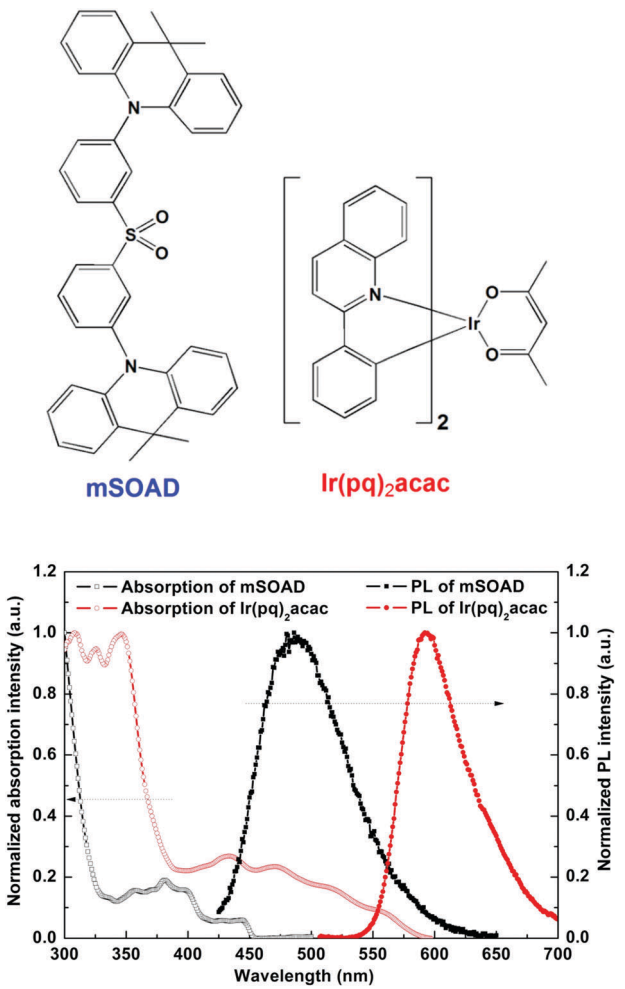

Fig. 1 The molecular structure, PL spectra and absorption spectra of mSOAD and $Ir(pq)_2acac$.

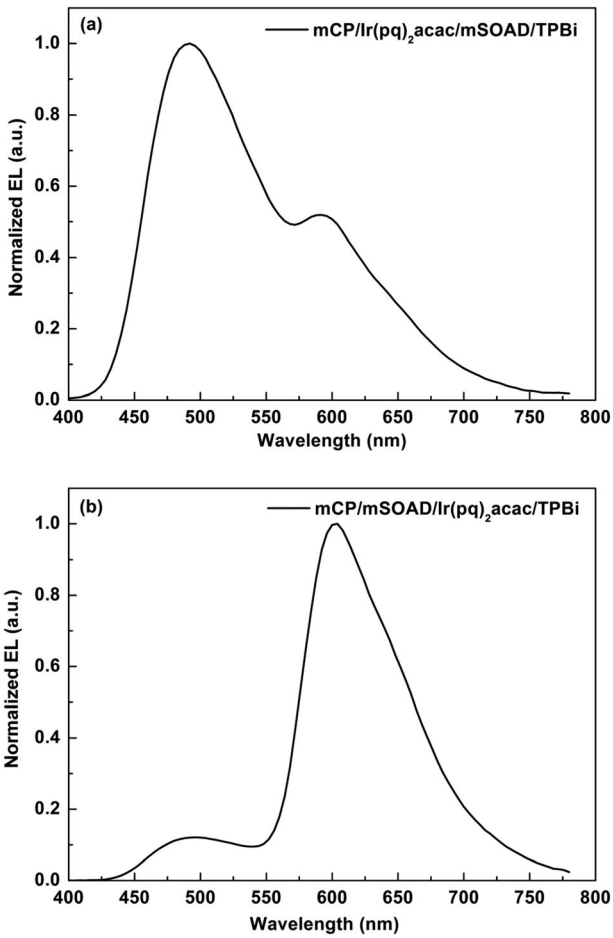

Fig. 2 The EL spectra of devices at 7 V. (a) ITO/MoO_3 (3 nm)/mCP (30 nm)/$Ir(pq)_2acac$ (~0.5 nm)/mSOAD (20 nm)/TPBi (40 nm)/LiF (1 nm)/Al. (b) ITO/MoO_3 (3 nm)/mCP (30 nm)/mSOAD (20 nm)/$Ir(pq)_2acac$ (~0.5 nm)/TPBi (40 nm)/LiF (1 nm)/Al.

were carried out at room temperature and under ambient conditions without any protective coatings.

3. Results and discussion

An mSOAD based acridine/sulfone derivative is designed and synthesized by our group by combining a diphenylsulfone core with bi-9,9-dimethyl-9,10-dihydroacridine substituted at the 3,3′-positions, which is a blue fluorescent emitter with an emission peak around ~490 nm. The molecular structure, PL spectra and absorption spectra of mSOAD and $Ir(pq)_2acac$ are shown in Fig. 1. The synthetic route and other thermal, optical and characterization data of mSOAD are described in another of our papers.[22] A large overlap between the PL of mSOAD and absorption of $Ir(pq)_2acac$ could be observed, which indicates that a highly efficient energy transfer from mSOAD to $Ir(pq)_2acac$ could occur. The PL spectra of mSOAD and $Ir(pq)_2acac$, which have emission peaks around ~490 nm and ~600 nm, respectively, also demonstrate that white light-emission could be achieved by employing two complementary colors.

In order to confirm the carrier transport characteristics of mSOAD and the location of the exciton recombination zone, we design firstly the device structure as follows: ITO/MoO_3 (3 nm)/mCP (30 nm)/$Ir(pq)_2acac$ (~0.5 nm)/mSOAD (20 nm)/TPBi (40 nm)/LiF (1 nm)/Al and ITO/MoO_3 (3 nm)/mCP (30 nm)/mSOAD (20 nm)/$Ir(pq)_2acac$ (~0.5 nm)/TPBi (40 nm)/LiF (1 nm)/Al. The *m*-bis(*N*-carbazolyl)benzene (mCP) and 1,3,5-tris(*N*-phenyl-benzimidazol-2-yl)benzene (TPBi) are the hole and electron transport layers, respectively. mSOAD and $Ir(pq)_2acac$ act as blue and red emitters, respectively. The EL spectra of the two devices are displayed in Fig. 2. Strong blue light-emission is observed when $Ir(pq)_2acac$ is in front of the mSOAD layer, while strong red light-emission from $Ir(pq)_2acac$ appears when it is at the back of the mSOAD layer. The results suggest that the exciton recombination zone is at the interface of mSOAD/TPBi. In the meantime, strong recombination emission at the mSOAD/TPBi interface could also confirm the good hole transport capability of mSOAD. Because if mSOAD exhibits better electron transport capability, the strong red light-emission of $Ir(pq)_2acac$ could be observed when $Ir(pq)_2acac$ is in front of the mSOAD layer. The ultra-thin red emitter is like a probe to indicate the recombination zone at the interface of mSOAD/TPBi, which also confirms that the hole transport capability is preferable to the electron transport capability in the mSOAD material. Then we combine the ultra-thin red emitter (~0.5 nm) and the mSOAD blue light-emitting layer to construct a series of non-doped WOLEDs by tuning the location and quantity of ultra-thin $Ir(pq)_2acac$ emitters in the devices.

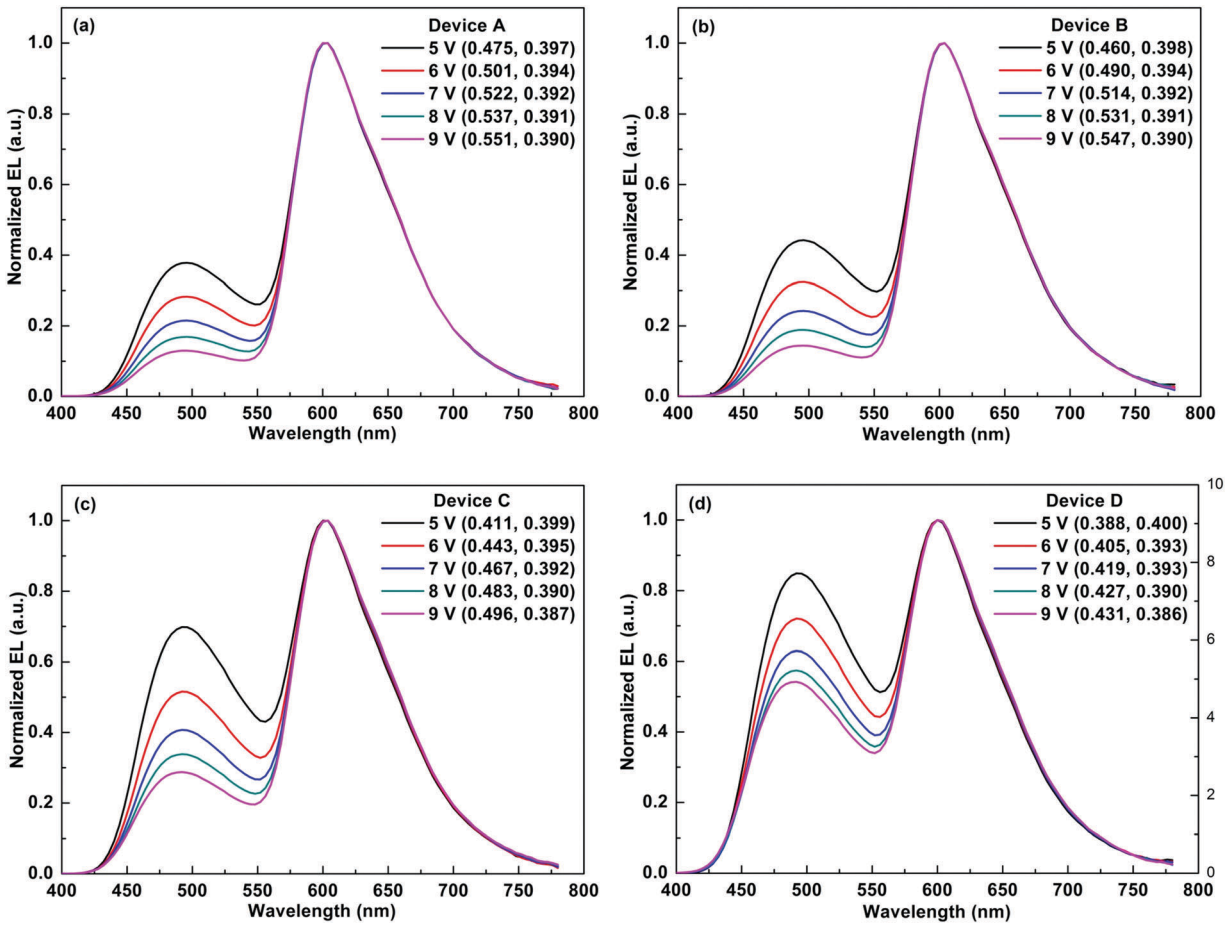

Fig. 3 The EL spectra of Device A–Device D from the operation voltage 5 V to 9 V. (a) Device A. (b) Device B. (c) Device C. (d) Device D.

Based on the good hole transport capability of mSOAD and the exciton recombination zone at the interface of mSOAD/TPBi, we insert firstly the single ultra-thin phosphorescent emitter into the interface and the electron transport layer (ETL) of TPBi to study the influence of ultra-thin emitter location on device performance. The WOLEDs designed are based on the non-doped device structure mentioned above: ITO/MoO_3 (3 nm)/mCP (30 nm)/mSOAD (20 nm)/TPBi (x nm)/Ir(pq)$_2$acac ($\sim$0.5 nm)/TPBi (40 $-$ x nm)/LiF (1 nm)/Al. The x = 0, 2, 4 and 6, are denoted as Device A, Device B, Device C and Device D, respectively. The key device structure parts are also shown in Fig. 4a. The EL spectra of Device A–Device D under different voltages are shown in Fig. 3. We can see that all the devices achieve white light-emission with two emission peaks of $\sim$470 nm from mSOAD and $\sim$600 nm from Ir(pq)$_2$acac. Moreover, when the ultra-thin phosphorescent emitter shifts from the interface of mSOAD/TPBi to the TPBi layer, the blue intensity is enhanced gradually, which indicates the existence of energy transfer from mSOAD to Ir(pq)$_2$acac. The singlet and triplet exciton energies of mSOAD (S_1 = 2.92 eV, T_1 = 2.9 eV) are higher than the triplet exciton energies of TPBi (T_1 = 2.74 eV) and Ir(pq)$_2$acac (T_1 = 2.1 eV), which ensures the occurrence of efficient energy transfer. The energy transfer efficiency decreases because of the increased distance when the Ir(pq)$_2$acac emitter moves away from the mSOAD layer gradually, which results in the enhancement of blue light-emitting intensity. But the color stability is poor with the increase of voltage. The blue light-emitting intensity decreases gradually with the increase of voltage because of the invalid confinements of TPBi to holes and excitons, which may induce the recombination zone shift from the interface to the TPBi layer, and even produce the TPBi excitons and then transfer to the phosphorescent emitter. So more and more exciton energies are transferred to low energy red emitters and result in the reduced blue emission intensity with increasing voltage. Although the location of the ultra-thin emitter in the TPBi layer could change the shape of the white light-emitting spectra, the poor color stability with increasing voltage should be improved further.

The EL efficiencies of Device A–Device D are shown in Fig. 4. The maximum EQEs of the four devices are 16.8%, 20.1%, 16.9% and 15.5%, respectively. A very high EQE above 20% is achieved with Device B; the corresponding current efficiency and power efficiency reach 36.6 cd A^{-1} and 30.0 lm W^{-1}, respectively. The high efficiency could be attributed to the fact that the 2 nm thin TPBi layer reduces the exciton concentration to some degree and balances the blue and red light-emitting intensity. While severe exciton concentration quenching may

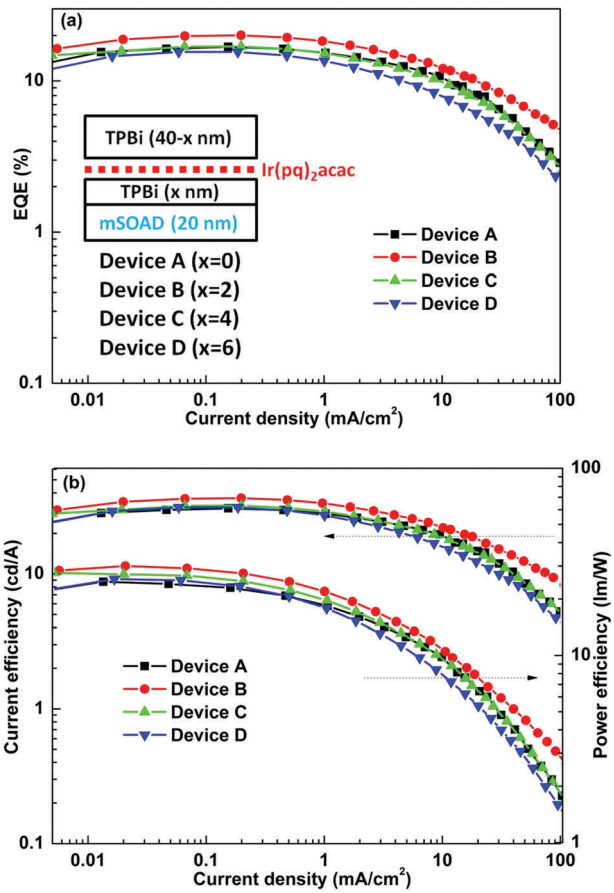

Fig. 4 The EL efficiencies of Device A–Device D. (a) The EQE–current density curves; inset shows the key device structure parts. (b) The current efficiency–current density–power efficiency curves.

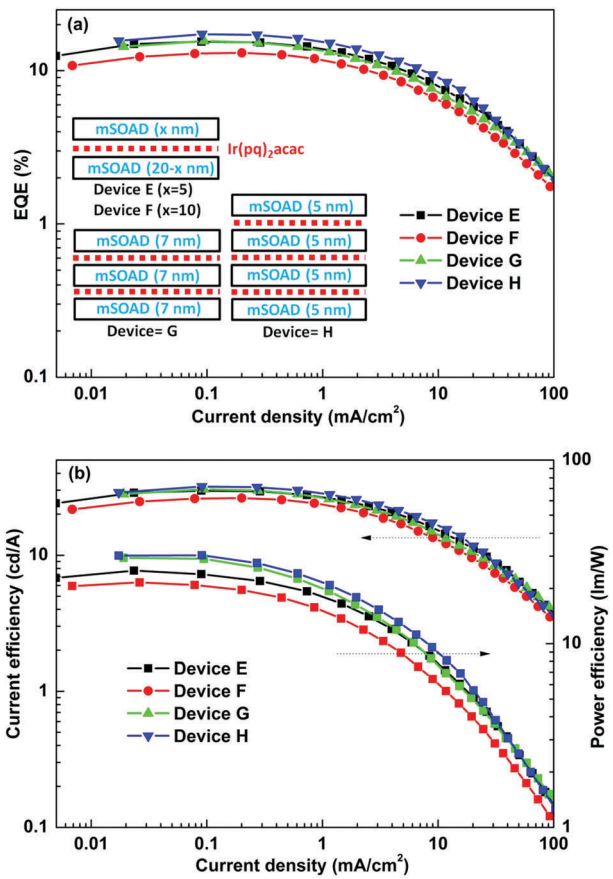

Fig. 5 The EL efficiencies of Device E–Device H. (a) The EQE–current density curves; inset is the EML structures. (b) The current efficiency–current density–power efficiency curves.

happen when $Ir(pq)_2acac$ is inserted into the interface of mSOAD/TPBi because of the formation of numerous excitons and radiative transition at the interface.[12,23] But the thicker TPBi layer in Device C and Device D decreases the number of excitons that could be transferred to $Ir(pq)_2acac$, which leads to low device efficiency. Therefore, the location of the ultra-thin emitter would have a large influence on the device efficiency and high efficiency could be realized by locating the ultra-thin emitter in the 2 nm TPBi layer away from the mSOAD/TPBi interface.

In order to prevent the exciton energy loss to the TPBi layer and further study the influence of ultra-thin emitters on device efficiency and white light-emitting spectra, we design another series of non-doped device structures with different locations and quantities of ultra-thin emitters as follows: ITO/MoO_3 (3 nm)/mCP (30 nm)/EML/DPEPO (2 nm)/TPBi (40 nm)/LiF (1 nm)/Al. The EML structures are shown in the inset of Fig. 5a. Device E–Device F are designed to further study the effect of single emitter location, while the influence of ultra-thin emitter quantity on device performance is explored in Device G–Device H. Bis(2-(diphenylphosphino)phenyl)ether oxide (DPEPO) is applied to the exciton block layer to confine excitons in the mSOAD layer due to the ultra-high singlet and triplet exciton energy (S_1 = 3.94 eV, T_1 = 2.98 eV).[24–26] The EL efficiencies of Device E–Device H are shown in Fig. 5. Device E (EQE: 15.4%) possesses a higher EQE than Device F (EQE: 13.1%), which demonstrates that higher efficiency could be achieved when the single ultra-thin emitter is located at a shorter distance to the mSOAD/DPEPO interface. The results are analogous to Device B–Device D with ultra-thin emitters in the TPBi layer. Device G–Device H realize higher efficiency, especially power efficiency, showing a larger improvement compared to Device E–Device F (Device G: 29.4 lm W^{-1}, Device H: 30.4 lm W^{-1} *vs.* Device E: 25.0 lm W^{-1}, Device F: 21.6 lm W^{-1}). The improvement of power efficiency stems from the lower turn-on voltage (~2.7 V *vs.* ~3.3 V), shown in Fig. S1 and S2 (ESI†), which further results from the better carrier recombination properties because of the higher current density at the same voltage shown in Fig. S2 (ESI†). The higher efficiency of Device G–Device H than that of Device E–Device F, especially the power efficiency, illustrates that more ultra-thin emitters contribute to improve the energy transfer efficiency and recombination efficiency. Device H with three ultra-thin phosphorescent emitters achieves the maximum current efficiency, power efficiency and EQE of 31.9 cd A^{-1}, 30.4 lm W^{-1} and 17.3%, respectively. The sufficient energy transfer could be realized in Device H due to the uniform distribution of the three emitters in the mSOAD layer. The application of a small quantity of ultra-thin emitters in a non-doped system helps in simplifying the fabrication process and improves the repeatability compared to

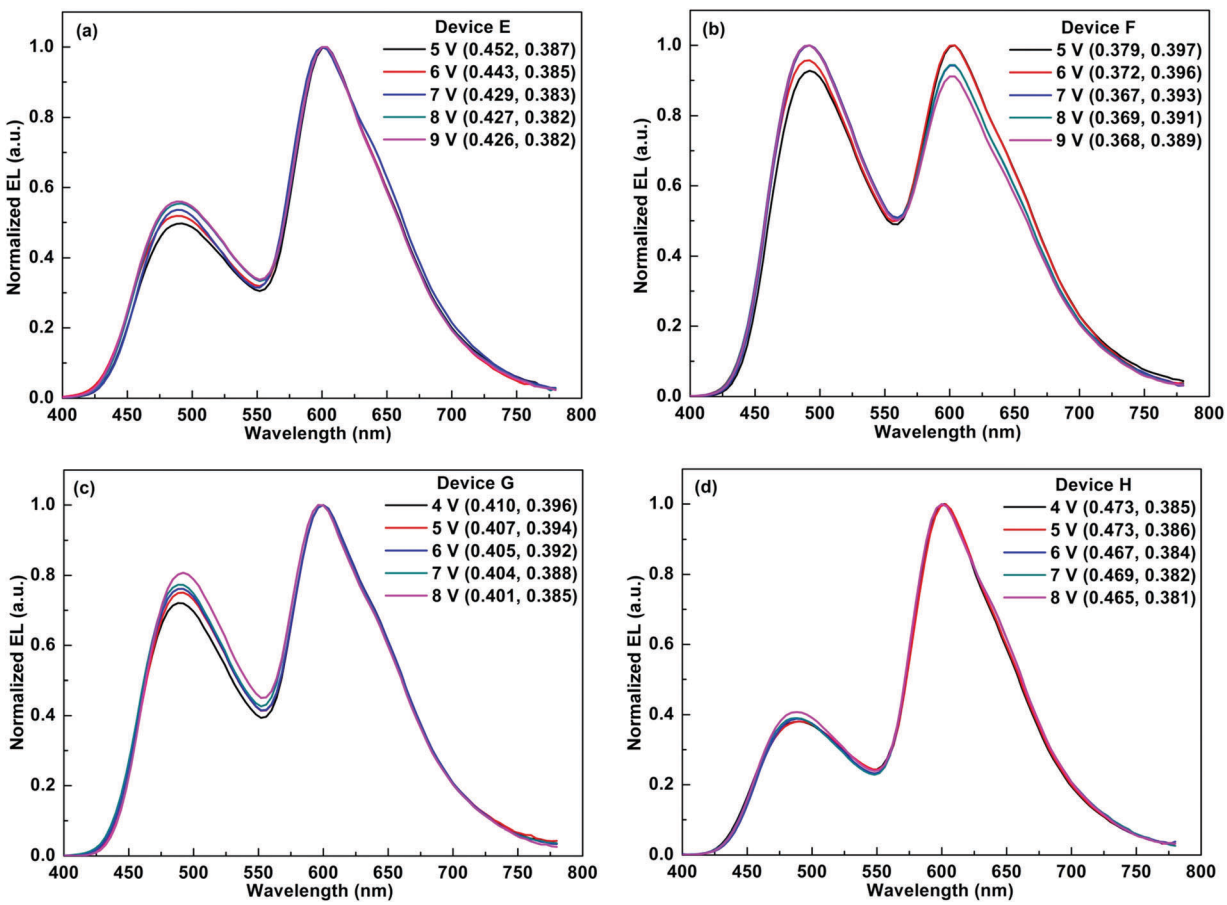

Fig. 6 The EL spectra of Device E–Device H under various voltages. (a) Device E. (b) Device F. (c) Device G. (d) Device H.

Table 1 Summary EL performances of all the WOLEDs in this paper

	$\eta_{c,Max.}/\eta_{p,Max.}/EQE_{Max.}$ [a] [cd A^{-1}/lm W^{-1}/%]	$\eta_{c,1000}/\eta_{p1000}/EQE_{1000}$ [b] [cd A^{-1}/lm W^{-1}/%]	$EQE_{Max.}$–EQE_{1000} [c] [%]	CIE/CRI [7 V]	ΔCIE coordinates
Device A	30.7/24.7/16.8	23.1/12.9/12.7	24	(0.522, 0.392)/67	(±0.076, ±0.007)
Device B	36.6/30.0/20.1	27.9/15.6/15.2	24	(0.514, 0.392)/69	(±0.087, ±0.008)
Device C	32.2/27.6/16.9	23.0/13.0/12.1	28	(0.467, 0.392)/76	(±0.085, ±0.012)
Device D	31.2/25.5/15.5	19.5/10.6/9.7	37	(0.419, 0.393)/80	(±0.043, ±0.014)
Device E	29.7/25.0/15.4	19.2/10.8/10.0	35	(0.429, 0.383)/78	(±0.026, ±0.005)
Device F	26.3/21.6/13.1	15.1/7.5/7.5	42	(0.367, 0.393)/79	(±0.011, ±0.008)
Device G	30.5/29.4/15.6	18.1/10.7/9.2	41	(0.404, 0.388)/79	(±0.009, ±0.011)
Device H	31.9/30.4/17.3	21.1/12.9/11.5	33	(0.469, 0.382)/73	(±0.008, ±0.004)

[a] Maximum current efficiency (η_c), power efficiency (η_p) and EQE. [b] η_c, η_p and EQE at 1000 cd m^{-2}. [c] EQE roll-off ratio from maximum to 1000 cd m^{-2}.

the host–guest doped system. Although the large quantity of ultra-thin phosphorescent emitters (>3) may improve the efficiency further, in contrast it would increase the complexity of the devices and also breach our original design for the non-doped WOLEDs.

The EL spectra of Device E–Device H are shown in Fig. 6. In contrast to the poor color stability of Device A–Device D with ultra-thin emitters at the interface and the TPBi layer, all the white light-emitting EL spectra of Device E–Device H exhibit high color stability in a wide voltage range, which corresponds to the brightness from ~100 cd m^{-2} to 5000 cd m^{-2}. The high color stability could be explained by the existence of DPEPO which blocks the exciton leakage to the TPBi layer and all the excitons are well confined in the EML. When the single ultra-thin emitter is inserted into the mSOAD layer, Device F has a higher blue intensity than Device E, which demonstrates again that the exciton recombination zone is nearby the mSOAD/DPEPO interface. The farther distance to the interface results in the stronger blue intensity due to the decrease of energy transfer efficiency. However, for Device G–Device H with two and three ultra-thin emitters, respectively, the more ultra-thin emitters obtain the stronger red light-emitting intensity, which demonstrates that the more efficient energy transfer from mSOAD to $Ir(pq)_2acac$ could occur. The high color stability of Device E–Device H indicates that the location and quantity of ultra-thin emitters in the mSOAD layer have no large effect on the spectral stability and the high color stability at enhanced voltages is mainly derived from the efficient confinement to excitons.

The EL performances of all the WOLEDs in this paper are summarized in Table 1. Combining the efficiency and white light-emitting spectra, Device H possesses the best performance, with the high power efficiency of 30.4 lm W^{-1} and the EQE of 17.4%. Besides, Device H also achieves the stable white light-emitting spectra and the variation of CIE coordinates is only (±0.008, ±0.004) from 4 V to 8 V. We consider that the high exciton energies of mCP and DPEPO contribute to confine excitons in the EML and stabilize the light-emitting zone,[27,28] which are the reasons for the excellent device performance.

To further clarify the light-emitting mechanism of the best WOLEDs of Device H, the schematic diagram is plotted in Fig. 7. The highest occupied molecular orbital (HOMO) and lowest unoccupied molecular orbital (LUMO) energy levels of

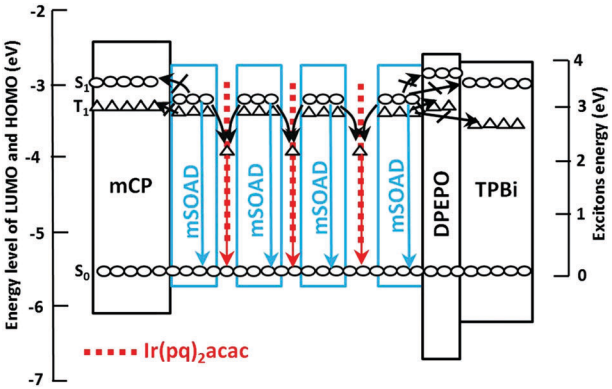

Fig. 7 The schematic diagram of white light-emitting mechanism in Device H.

mSOAD (HOMO: 5.76 eV, HOMO: 2.79 eV) are well confined between mCP (HOMO: 6.1 eV, LUMO: 2.4 eV) and DPEPO (HOMO: 6.8 eV, LUMO: 2.6 eV), which help to confine the injected electrons and holes in the EML and achieve a high recombination efficiency. Moreover, the singlet and triplet exciton energies of mCP (S_1 = 3.5 eV, T_1 = 3.0 eV) and DPEPO (S_1 = 3.94 eV, T_1 = 2.98 eV) are higher than that of mSOAD (S_1 = 2.92 eV, T_1 = 2.9 eV), so all the singlet and triplet excitons would also be confined in the EML, which results in high light-emitting efficiency. Although the triplet exciton energy of TPBi is lower than that of mSOAD as mentioned above, the introduction of DPEPO prevents successfully the leakage of mSOAD excitons. On the other hand, the HOMO and LUMO energy level and triplet excitons energy of $Ir(pq)_2acac$ (HOMO: 5.2 eV, LUMO: 3.1 eV, T_1 = 2.1 eV) are also well confined by mSOAD. Therefore, the high energy excitons produced on mSOAD would be transferred partly to the phosphorescent emitter through the Förster and Dexter process by controlling the quantity of ultra-thin phosphorescent emitters. The direct radiative transition of mSOAD singlet excitons and triplet excitons of $Ir(pq)_2acac$, transferred from mSOAD, produces white light-emission. We consider that carrier trapping may not exist due to the very few phosphorescent emitters and almost the same current density–voltage curves of the devices with two and three ultra-thin phosphorescent emitters,[29,30] which are shown in Fig. S2 (ESI†). Above all, the sufficient energy transfer from mSOAD to $Ir(pq)_2acac$ and the efficient confinement to carriers and excitons are responsible for the stable spectra and high efficiency of Device H.

4. Conclusion

A simple method is adopted to construct highly efficient and color stable non-doped WOLEDs. By modulating the location and quantity of ultra-thin phosphorescent emitters, high current efficiency, power efficiency and EQE of 31.9 cd A^{-1}, 30.4 lm W^{-1} and 17.3% are achieved, respectively. Moreover, a high color stability of ($\pm$0.008, $\pm$0.004) is also obtained simultaneously. The high energy transfer efficiency and efficient confinement to carrier and excitons are the main reasons for the excellent performance. The influence of ultra-thin emitters with different locations and quantities on device performance is also researched. Moreover, the non-doped technology provides a simple and high repeatability approach to construct highly efficient and color stable WOLEDs.

Conflicts of interest

There are no conflicts to declare.

Acknowledgements

This work was financially supported by the National Natural Science Foundation of China (61605137, 61605138, 61705156, 61775155 and 61704118); Scientific and Technological Innovation Programs of Higher Education Institutions in Shanxi (STIP, No. 2016134).

Notes and references

1 C. W. Tang and S. A. VanSlyke, *Appl. Phys. Lett.*, 1987, **51**, 913–915.
2 M. A. Baldo, D. F. O'Brien, Y. You, A. Shoustikov, S. Sibley, M. E. Thompson and S. R. Forrest, *Nature*, 1998, **395**, 151–154.
3 C. Adachi, M. A. Baldo, M. E. Thompson and R. F. Stephen, *J. Appl. Phys.*, 2001, **90**, 5048–5051.
4 H. Uoyama, K. Goushi, K. Shizu, H. Nomura and C. Adachi, *Nature*, 2012, **492**, 234–238.
5 C. Zheng, W. Zhao, Z. Wang, D. Huang, J. Ye, X. Ou, X. Zhang, C. S. Lee and S. T. Lee, *J. Mater. Chem.*, 2010, **20**, 1560–1566.
6 J. Huang, Y. Jiang, J. Yang, R. Tang, N. Xie, Q. Li, H. S. Kwok, B. Tang and Z. Li, *J. Mater. Chem. C*, 2014, **2**, 2028–2036.
7 Q. Zhang, D. Tsang, H. Kuwabara, Y. Hatae, B. Li, T. Takahashi, S. Y. Lee, T. Yasuda and C. Adachi, *Adv. Mater.*, 2015, **27**, 2096–2100.
8 J. Guo, X. Li, H. Nie, W. Luo, S. Gan, S. Hu, R. Hu, A. Qin, Z. Zhao, S. Su and B. Tang, *Adv. Funct. Mater.*, 2017, 1606458.
9 Y. H. Song, S. J. Yeh, C. T. Chen, Y. Chi, C. S. Liu, J. K. Yu, Y. H. Hu, P. T. Chou, S. M. Peng and G. H. Lee, *Adv. Funct. Mater.*, 2004, **14**, 1221–1226.
10 T. Xu, M. Yang, J. Liu, X. Wu, I. Murtaza, G. He and H. Meng, *Org. Electron.*, 2016, **37**, 93–99.
11 Y. Yin, J. Yu, H. Cao, L. Zhang, H. Sun and W. Xie, *Sci. Rep.*, 2014, **4**, 6754.
12 Y. Zhao, J. Chen and D. Ma, *ACS Appl. Mater. Interfaces*, 2013, **5**, 965–971.
13 T. Tan, S. Ouyang, Y. Xie, D. Wang, D. Zhu, X. Xu and H. H. Fong, *Org. Electron.*, 2015, **25**, 232–236.
14 Y. Miao, K. Wang, B. Zhao, L. Gao, P. Tao, X. Liu, Y. Hao, H. Wang, B. Xu and F. Zhu, *Nanophotonics*, 2018, **7**, 295–304.
15 T. Zhang, C. Shi, C. Zhao, Z. Wu, N. Sun, J. Chen, Z. Xie and D. Ma, *J. Mater. Chem. C*, 2017, **5**, 12833–12838.
16 F. Zhao, L. Zhu, Y. Liu, Y. Wang and D. Ma, *Org. Electron.*, 2015, **27**, 207–211.
17 L. Xu, C. W. Tang and L. J. Rothberg, *Org. Electron.*, 2016, **32**, 54–58.
18 S. J. Su, E. Gonmori, H. Sasabe and J. Kido, *Adv. Mater.*, 2008, **20**, 4189–4194.
19 T. Xu, Y. Zhang, B. Wang, C. Huang, I. Murtaza, H. Meng and L. Liao, *ACS Appl. Mater. Interfaces*, 2017, **9**, 2701–2710.
20 T. Xu, J. Zhou, C. Huang, L. Zhang, M. Fung, I. Murtaza, H. Meng and L. Liao, *ACS Appl. Mater. Interfaces*, 2017, **9**, 10955–10962.
21 B. Zhao, Y. Miao, Z. Wang, K. Wang, H. Wang, Y. Hao, B. Xu and W. Li, *Nanophotonics*, 2017, **6**, 1133–1140.
22 J. Li, R. Zhang, Z. Wang, B. Zhao, J. Xie, F. Zhang, H. Wang and K. Guo, *Adv. Opt. Mater.*, 2018, **6**, 1701256.
23 S. Wu, S. Li, Q. Sun, C. Huang and M. K. Fung, *Sci. Rep.*, 2016, **6**, 25821.
24 J. Zhang, D. X. Ding, Y. Wei and H. Xu, *Chem. Sci.*, 2016, **7**, 2870–2882.
25 J. H. Lee, S. H. Cheng, S. J. Yoo, H. Shin, J. H. Chang, C. I. Wu, K. T. Wong and J. J. Kim, *Adv. Funct. Mater.*, 2015, **25**, 361–366.
26 M. Kim, S. K. Jeon, S. H. Hwang and J. Y. Lee, *Adv. Mater.*, 2015, **27**, 2515–2520.
27 T. J. Park, W. S. Jeon, J. W. Choi, R. Pode, J. Jang and J. H. Kwon, *Appl. Phys. Lett.*, 2009, **95**, 103303.
28 Y. S. Park, J. W. Kang, D. M. Kang, J. W. Park, Y. H. Kim, S. K. Kwon and J. J. Kim, *Adv. Mater.*, 2008, **20**, 1957–1961.
29 C. Weichsel, L. Burtone, S. Reineke, S. I. Hintschich, M. C. Gather, K. Leo and B. Lüssem, *Phys. Rev. B: Condens. Matter Mater. Phys.*, 2012, **86**, 075204.
30 L. Zhu, Z. Wu, J. Chen and D. Ma, *J. Mater. Chem. C*, 2015, **3**, 3304–3310.

